Astrophysics and Space Science (2025) 370:47
https://doi.org/10.1007/s10509-025-04439-2

RESEARCH

Retrograde co-orbital motion with Jupiter. Periodic orbits and dynamical maps

George Voyatzis[1] · Thomas Kotoulas[1] · Maria Helena Moreira Morais[2]

Received: 12 March 2025 / Accepted: 7 May 2025 / Published online: 14 May 2025

Abstract
This study aims to provide comprehensive insights into the dynamics of retrograde co-orbital motion, contributing to our understanding of the origin and evolution of retrograde asteroids in the solar system. The paper studies retrograde co-orbital motion with Jupiter through the computation of symmetric periodic orbits in both planar and spatial circular restricted three-body problems. The research begins with an analysis of families of the planar circular problem at which there exist three main families of co-orbital motion. Starting from the vertical critical orbits of these families we extend our study to three-dimensional configurations, revealing that most spatial families exhibit instability. The phase-space structure is also explored by using dynamical stability maps under various initial conditions. These maps help identify regions of stable motion within predominantly chaotic domains. The theoretical framework is applied to asteroid (514107) Ka'epaoka'awela, demonstrating its chaotic nature with a Lyapunov time of approximately 6350 years, despite remaining in co-orbital resonance with Jupiter for many million years.

Keywords Asteroids · Retrograde orbits · Co-orbital motion · Three-body problem

1 Introduction

In the last two decades the dynamics of minor bodies of our solar system which move on retrograde orbits around the Sun drew the attention of many researchers since their origin is still a mystery. Up to now, more than 150 bodies have been discovered. The dynamical lifetimes of 25 retrograde asteroids were studied by (Kankiewicz and Wlodarczyk 2017, 2018). Their results revealed that stability is possible over the age of the solar system. From the perspective of dynamics, it is interesting that many retrograde asteroids are in mean motion resonances (MMRs) with a major planet (Morais and Namouni 2013a; Li et al. 2019). For instance, the dynamical evolution of the first nearly-polar trans-Neptunian object 471325 Taowu in 1/-3 MMR with Neptune and the asteroid 514107 Káepaokáawela in 1/-1 MMR with Jupiter were studied by Morais and Namouni (2017b) and Namouni and Morais (2018b), respectively.

Greenstreet et al. (2012) studied numerically the evolution of main belt objects that become Near Earth Asteroids and showed that retrograde orbits may result from the action of MMRs. The dynamics of MMRs in the model of the restricted three body problem (RTBP) is associated with periodic orbits but most studies in the past refer to prograde motion. Families of spatial periodic orbits that extend from planar prograde orbits to planar retrograde orbits (i.e. $0 < i < 180°$) have been computed (Jefferys and Standish 1972; Ichtiaroglou et al. 1989) but their stability is not studied. Morais and Namouni (2013b) investigated the phase-space structure in the case of the main retrograde resonances (2/-1, 1/-1, 1/-2) applying the method of surface of section and by using a suitable disturbing function for the nearly planar problem. Analytical or semi-analytical models based on disturbing functions which are valid for arbitrary inclination have been proposed (Namouni and Morais 2018a; Lei 2019; Gallardo 2020; Namouni and Morais 2020). For the asteroid

✉ T. Kotoulas
tkoto@physics.auth.gr

G. Voyatzis
voyatzis@auth.gr

M.H.M. Morais
helena.morais@unesp.br

1 Department of Physics, Aristotle University of Thessaloniki, University Campus, Thessaloniki, 54124, Greece

2 Instituto de Geociências e Ciências Exatas, Universidade Estadual Paulista (UNESP), Av. 24-A, Rio Claro, 1515 13506-900, SP, Brazil

belt, a complete study of families of retrograde symmetric periodic orbits (planar or three-dimensional) was done by Kotoulas and Voyatzis (2020a) and Kotoulas et al. (2022b). As far as the Kuiper-belt is concerned, analogous studies are given in Kotoulas and Voyatzis (2020b) and Kotoulas et al. (2022a).

The present study focuses on the study of retrograde co-orbital motion (1/-1 MMR) with Jupiter in the model of RTBP. Huang et al. (2018) studied the dynamics of the planar retrograde 1/-1 MMR by using an averaged model. Morais and Namouni (2016) explored the dynamics of the coorbital resonance for the whole interval of inclination (0 <i< 180°) in the circular RTBP and examined the similarities and differences between planar and the three-dimensional resonance capture. Also, in Morais and Namouni (2019) they studied planar and three-dimensional symmetric retrograde periodic orbits connecting them with possible capture of asteroids in co-orbital motion with Jupiter. The study of such a resonance is not only interesting from a theoretical point of view but also due to existence of the asteroid Káepaokáawela, which is a special sample that could help explain the origin of retrograde asteroids (Namouni and Morais 2018c).

In Sect. 2 we describe the structure of families of planar periodic orbits of co-orbital motion and find the bifurcation points from which families of three dimensional (3D) periodic orbits are analytically continued with parameter the inclination. These families are presented in Sect. 3. In Sect. 4 dynamical stability maps are computed in order to study the structure of the phase space in the region of co-orbital motion. Section 5 studies the dynamical features of the evolution of 514107 Ka'epaoka'awela and, finally, we conclude in Sect. 6.

2 Co-orbital planar retrograde motion

We consider the planar circular RTBP in a rotating frame Oxy with the primaries, Sun and Jupiter (of masses $1-\mu$ and μ =0.001, respectively), to be located on the Ox axis, where the origin O is the center of mass. The system possesses only one integral, the Jacobi constant, C (Murray and Dermott 1999)

$$C = -(\dot{x}^2+\dot{y}^2)+x^2+y^2+2\left(\frac{1-\mu}{r_1}+\frac{\mu}{r_2}\right),$$

where $r_1^2=(x+\mu)^2+y^2$ and $r_2^2=(x-1+\mu)^2+y^2$. We note that for 1/1 MMR Trojan asteroids is $C\approx 3$, while for retrograde asteroids, studied in this paper, is about $-1.2 < C < 0$. Considering an inertial frame, which at $t=0$ coincides with the rotating one, we can define the osculating orbital elements to the massless body (asteroid), namely, the semimajor axis (a), the eccentricity (e), the pericenter longitude(ϖ) and the mean anomaly (M). In this frame the elements for Jupiter are a' =1, e' =0, $M'=0$ and $\varpi'=0$. For the MMR 1/-1 (co-orbital motion) we consider the resonant angle (Morais and Namouni 2013b)

$$\phi=\lambda-\lambda'-2\varpi, \tag{1}$$

where λ, λ' are the mean longitudes of asteroid and of the planet, respectively and the main types of periodic orbits are categorized as (Morais and Namouni 2019)

- Circular orbits ($e\approx 0$). We call them orbits of *mode-0* and can be interior (a <1) or exterior (a >1).
- Elliptic orbits that pass alternately inside or outside the orbit of Jupiter at its perihelion and ϕ librates around 0° (*mode-1*).
- Elliptic orbits of large eccentricity, $e\gtrsim 0.7$, (interior or exterior), the angle ϕ librates around 180° (*mode-2*).
- Elliptic orbits of small eccentricity, $e\lesssim 0.3$, (interior or exterior), the angle ϕ librates around 180° (*mode-3*).

Samples of these orbits are presented in Fig. 1.

Periodic orbits of all modes are symmetric with respect to the axis $y=0$, which are the most common periodic orbits in the circular planar RTBP (Hadjidemetriou and Ichtiaroglou 1984; Hénon 1997). Except for circular orbits, the orbits are of double multiplicity i.e. they perform two revolutions in the rotating frame in one period. In our extensive study we did not identify existence of asymmetric retrograde co-orbital motion. We remark that asymmetric periodic orbits exists for exterior prograde MMRs of the form $1/n$, $n=2,3,\dots$ (Beaugé 1994). Due to the symmetry, periodic motion corresponds to initial conditions (x_0, $y_0=0$, $\dot{x}_0=0$, $\dot{y}_0$) and satisfy the periodicity conditions $y(\frac{T}{2})=\dot{x}(\frac{T}{2})=0$, where T is the period of the orbit. Periodic orbits of each mode form monoparametric families with parameter the Jacobi constant C, which can be presented as characteristic curves in various planes. In Fig. 2 we present the families in the plane (a_0, C), where the semimajor axis a_0 is computed at the initial conditions of the periodic orbit with $x_0<0$ for the modes 0, 2, and 3 (i.e. at the far side from Jupiter). For mode-1 there are two perpendicular sections for $x_0>0$ (see Fig. 1f), and we choose the section for $x_0>1$.

As it was indicated by Hadjidemetriou (1988), the family of retrograde circular orbits of the unperturbed problem ($\mu=0$), is continued for $\mu\neq 0$ as a family, denoted by R_C, with orbits nearly circular and stable. However, the family R_C breaks at 1/-1 MMR and is separated into two branches, the interior branch R_C^{in} and the exterior one R_C^{ext}. Also as the 1/-1 MMR is approached, the circular orbits become unstable (either horizontally or vertically). The linear stability of the orbits is indicated along the characteristic curves with different colors (see legend of Fig. 2). The points where stability changes, A_1,B_i and S_i ($i=1..3$), consist bifurcation

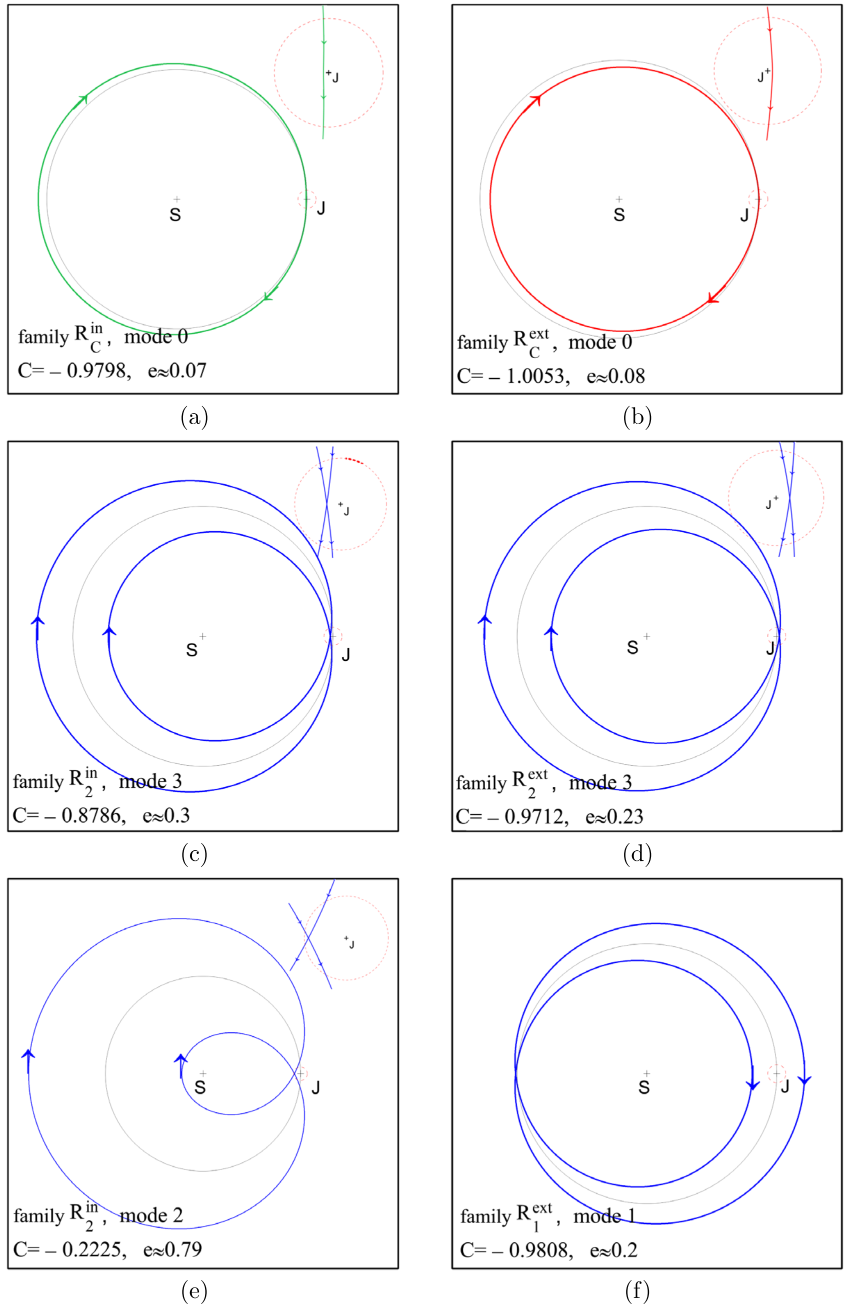

Fig. 1 Samples of Periodic orbits of different modes in the rotating frame. Color indicates their stability type and R the family where they belong to (see Fig. 2). A maginification around Jupiter is given in the inset panels

points. The bifurcation point S_0 (at $a_0 = 0.9266$) is the point where the interior branch of the circular family becomes unstable. This point is quite far from $a = 1$ and the bifurcated family R_0^{in} of unstable orbits is not considered as being in the 1/-1 MMR. At the point S_1 (see also the magnification in Fig. 3) we obtain a period doubling and the generation of the interior family R_2^{in} which starts with stable orbits (mode-3). Then an unstabe segment follows up to $C = -0.9562$ (or $e = 0.02315$), where the orbits becomes stable again giving the highly eccentric co-orbital motion (mode-2). A similar bifurcation occurs at the point S_2 of the exterior circular family generating co-orbital motion of mode-3 up to $C = -1.03868$ (or $e = 0.02556$). As C increases, these orbits become strongly unstable and continuation brakes. So, no exterior co-orbital motion of mode-2 is found. The rest bifurcation points on the circular family, A_1, B_1, B_2 and B_3 are vertical critical orbits (v.c.o.) and generate families of three dimensional orbits (Hénon 1973), which are discussed in the next section. Family R_1 consists of orbits of mode-1 that intersects the Ox axis twice, for $x_0 < 1$ and $x_0 > 1$. In the region of 1/-1 resonance only the v.c.o. B_4 exists.

The computed families have been also given by Morais and Namouni (2019) in a different perspective. In the framework of the planar elliptic RTBP, families of co-orbital mo-

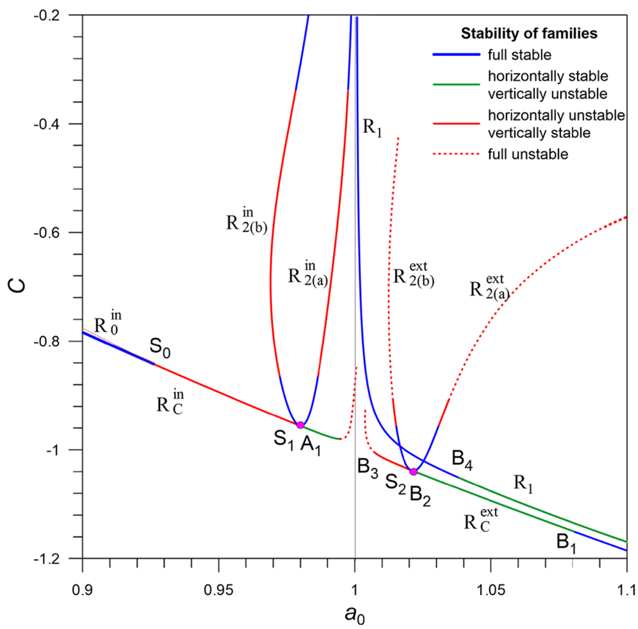

Fig. 2 Families of periodic orbits in the vicinity of 1/-1 MMR with Jupiter. The two branches, a and b, of families R_2^{in} and R_2^{ext} consist of the same orbits. Different colors refer to different types of linear stability as it is indicated in the figure legend. The points A_1, B_i and S_i $(i=1..3)$ are bifurcation points as it is described in the text

tion are presented in Voyatzis and Kotoulas (2024). Generally speaking, for co-orbital motion the horizontally unstable periodic orbits are surrounded by strongly chaotic motion which leads either to collisions (mainly with Sun) or escape.

3 Families of retrograde periodic orbits in the 3D circular RTBP

Considering Jupiter in circular motion, we shall present below families of 3D retrograde symmetric periodic orbits at 1/-1 resonance. Many of these families are also studied by Morais and Namouni (2019) but here we provide a different presentation clarifying their starting and termination points. As in the planar case, periodicity refers to the rotating frame $Oxyz$. According to symmetries of the spatial circular RTBP we have two types of symmetric periodic orbits (Kotoulas et al. 2022b,a):

Type F: The periodic orbits have symmetry with respect to xz-plane with initial conditions: $x_0,\ y_0=0,\ z_0,\ \dot{x}_0=0,\ \dot{y}_0,\ \dot{z}_0=0$, and the periodicity conditions are: $y(\frac{T}{2})=0,\ \dot{x}(\frac{T}{2})=0,\ \dot{z}(\frac{T}{2})=0$,

Type G: The periodic orbits are symmetric with respect to x-axis with initial conditions: $x_0,\ y_0=0,\ z_0=0,\ \dot{x}_0=0,\ \dot{y}_0,\ \dot{z}_0$, and the periodicity conditions are: $y(\frac{T}{2})=0,\ z(\frac{T}{2})=0,\ \dot{x}(\frac{T}{2})=0$.

Starting from a planar v.c.o. we set $z(0)=\delta z \ll 1$ (for type F) or $\dot{z}(0)=\delta\dot{z} \ll 1$ (for type G) and we perform differential corrections in order to satisfy the periodicity conditions. Repeating this process we have the analytical continuation of solutions and construct the 3D families (see Lara and Peláez 2002; Kalantonis 2020). Thus, a periodic orbit having symmetry of type F or type G can be represented by a point in the 3D space of initial conditions $(x_0, z_0, \dot{y}_0)$ or $(x_0, \dot{y}_0, \dot{z}_0)$, respectively. However, the presentation of the orbits by their initial osculating elements $(a_0,\ e_0,\ i_0)$ is preferable. Since we study periodic orbits near a mean motion resonance, the semimajor axis is almost constant but the eccentricity and the inclination vary along a family. The linear stability of periodic motion is identified by the two pairs of non unit reciprocal eigenvalues of the monodromy matrix. Orbits are stable when all eigenvalues are on the unit circle, simply unstable when one pair of eigenvalues is on the real axis and doubly unstable when both pairs are on the real axis (Broucke 1969). The case of complex instability, i.e. when eigenvalues are out of the unit circle but not on the real axis, has not been found for co-orbital periodic motion.

As we mentioned above, families of 3D periodic orbits bifurcate from v.c.o. which have been indicated in Fig. 2. The orbital elements and the Jacobi constant of the v.c.o. found and the families which bifurcates from them are shown in Table 1. For the retrograde 1/-1 MMR we can define the resonant angles (Morais and Namouni 2016; Namouni and Morais 2018a)

$$\phi_k = \lambda - \lambda' - k\omega \tag{2}$$

where $\lambda = M + \varpi$, $\lambda' = M' + \varpi'$ are the mean longitudes of the asteroid and the Jupiter, respectively. The resonant angles (for $k=0,2$) which correspond to the 3D periodic orbits of the families are also indicated in Table 1.

The interior planar family (R_C^{in}) has one v.c.o. denoted by A_1. Family R_{A1}, which bifurcates from this point, is doubly symmetric, which means that has both types of symmetry, F and G. Along the family, the inclination decreases monotonically and the family terminates at $i=0°$ to the Lagrangian point L_1. Actually, this family is the family of vertical Lyapunov orbits emanating from L_1 (Hou and Liu 2009). It is whole unstable and its characteristic curves are shown in Fig. 4.

Regarding the planar family R_C^{ext}, we have the three v.c.o., B_i, $i=1,2,3$. Family R_{B1} is of type G and starts from the point B_1 with stable orbits. At the point G_1 (at $i=172.76°$) the stability type changes and the family becomes simply unstable (see Fig. 5). A new unstable family of three-dimensional periodic orbits, R_{B4}, bifurcates from this point and terminates to the point B_4. There are two more points at which the stability type of the family R_{B1} changes (see Fig. 5a,b): $G_2(i=145.69°)$, where the orbits from simply ustable become doubly unstable, and G_3 $(i=119.89°)$

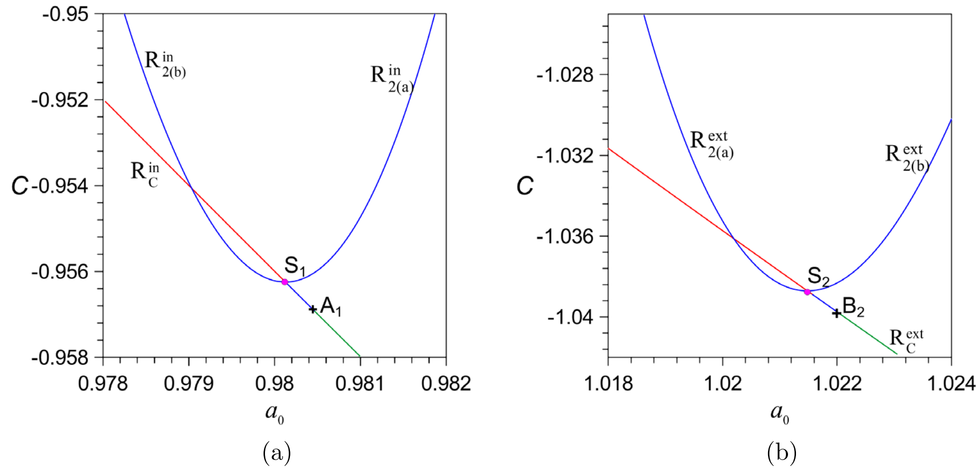

Fig. 3 Families of retrograde periodic orbits in the 1/-1 MMR presented on the planes $a_0 - C$ (left: interior orbits and right: exterior orbits). The linear stability is indicated by different colors as in Fig. 2

Table 1 V.C.Os and families of orbits

v.c.o	Jacobi (C)	a	e	name	angles (ω, Ω, M, ϕ_0, ϕ_2)	D(e_0^*, i_0^*)
A_1	-0.956976	0.980492	0.0235	R_{A1}	($\frac{3\pi}{2}$, $\frac{3\pi}{2}$, π, 0, π)	
B_1	-1.149941	1.080381	0.0078	R_{B1}	(0, π, 0, π, π)	D(0.000, 65.468)
B_2	-1.039463	1.021857	0.0251	R_{B2}	($\frac{\pi}{2}$, $\frac{3\pi}{2}$, 0, 0, π)	
B_3	-1.004731	1.007253	0.0823	R_{B3}	($\frac{\pi}{2}$, $\frac{3\pi}{2}$, 0, 0, π)	
B_4	-1.050709	1.038026	0.1125	R_{B4}	($\frac{3\pi}{2}$, $\frac{\pi}{2}$, π, π, 0)	

[1]The point D(e_0^*, i_0^*) indicates the point where one (at least) of the angle variables of the family R_{B1} changes value

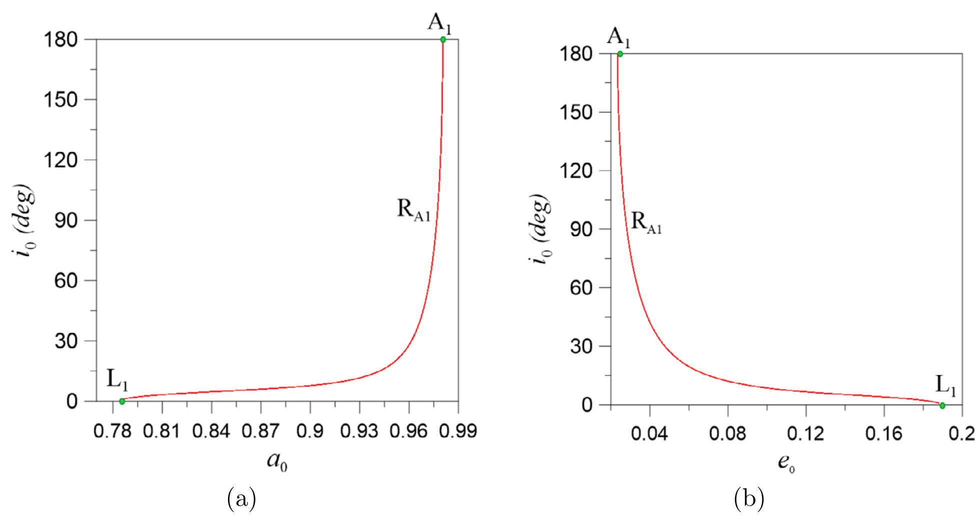

Fig. 4 Family R_{A1} of 3D retrograde symmetric periodic orbits in the 1/-1 MMR presented on the planes $a_0 - i_0$ (left) and $e_0 - i_0$ (right). All orbits are simply unstable

where the orbits becomes again simply unstable. A new family, R_{G3}, bifurcates from the point G_3 and terminates to a direct orbit of the planar problem ($e = 0.908$, $i = 0°$) as it is shown in Fig. 6. All orbits of R_{G3} are doubly unstable. At the point G_4, where we have an almost circular orbit ($e_0 = 0$) the argument of perihelion (ω) changes from 0 to π but the family remains unstable and terminates to the Lagrangian point L_3.

Family R_{B2} bifurcates from the point B_2 and terminates to the Lagrangian point L_2. It is presented in Fig. 7 and consists of simply unstable orbits for $180° < i_0 < 178.48°$ and doubly unstable for $178.48° < i_0 < 6.23°$. Finally, it becomes again simple unstable and terminates to the Lagrangian point L_2. From the bifurcation point at $i_0 = 178.48°$ another family of type F bifurcates and is denoted as R_{H1}. This family is simply unstable but becomes stable

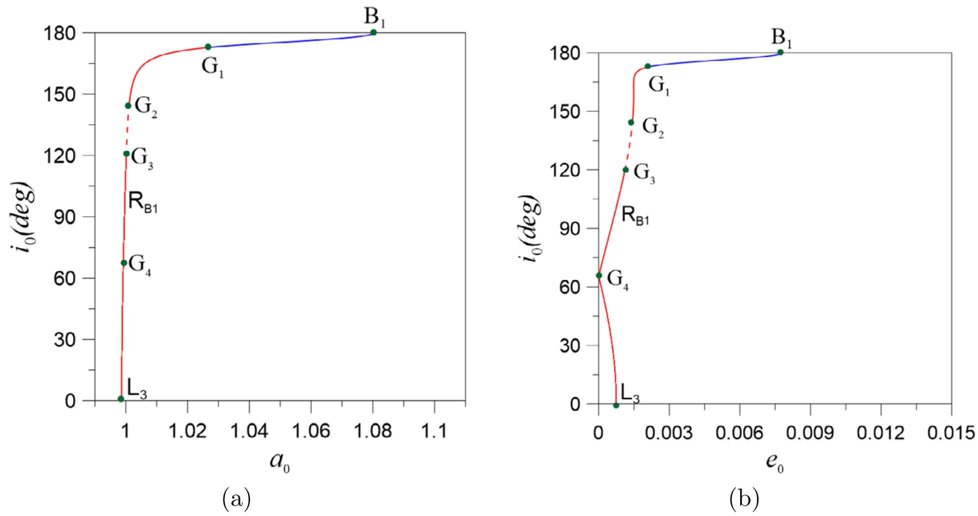

Fig. 5 Characteristic curves of the family R_{B1} presented on the planes (a) $a_0 - i_0$ and (b) $e_0 - i_0$ on the same plane (right). Blue lines, red solid lines and dashed red lines correspond to stability, simple instability and double instability, respectively

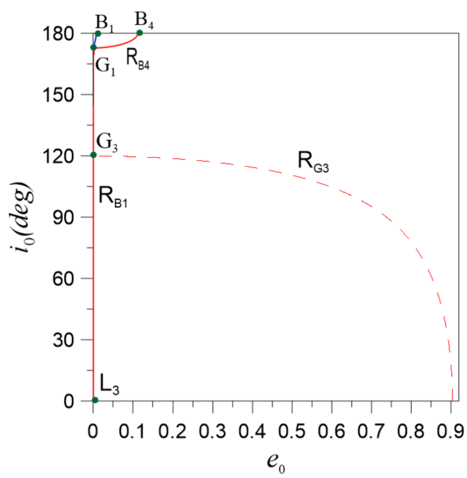

Fig. 6 c) Characteristic curves $e_0 - i_0$ of the families R_{B4} and R_{G3}. Colors indicate stability as in Fig. 5

for $e_0 > 0.892$ and seems to terminate to a collision orbit with Sun ($e_0 \to 1$).

From the third v.c.o., B_3, family R_{B3} bifurcates having simply unstable orbits. At about $i_0 = 100°$ orbits becomes very unstable and continuation breaks (see Fig. 8).

4 Dynamical stability maps

Apart from a small segment of the family R_{B1} which consists of stable orbits in the interval $173° < i_0 < 180°$, all other periodic orbits found are unstable with chaotic orbits in their neigbourhood. In order to examine the orbital stability in wider regions in phase space, we compute dynamical maps based on the fast Lyapunov indicator (FLI) Froeschlé et al. (1997). Particularly we compute the de-trended indicator (DFLI) defined as (Voyatzis 2008):

$$DFLI(t) = sup_{0<\tau\leq t} \log\left[\frac{1}{\tau}\frac{\xi(\tau)}{\xi(0)}\right], \tag{3}$$

where ξ is the norm of the deviation vector computed after numerical integration of the variational equations along the orbit. The FLI grows linearly in time for regular orbits but the de-trended one tends to a small constant value along the integration. Both indicators grow exponentially in case of chaotic orbits. For the computations of the dynamical maps we considered the elliptic RTBP with Jupiter's elements $a' = 1$, $e' = 0.048$, $\varpi' = 0$ and $M'(0) = 0$. The grids of initial conditions (of size 200×200) are defined in the plane $a - e$ while the rest initial orbital elements are set as constants for a particular grid. They are selected such that to represent orbits of the mode 2,3 and mode 1. Each orbit has been integrated for 8000 revolutions of the Jupiter or until DFLI< 30. Dark regions in the maps correspond to low DFLI values (stability) while yellow colored regions indicate strong chaotic evolution. The main stable regions on the dynamical maps are indicated by capital letters and according to the libration of the argumernt of pericenter and the resonant angles as it is shown in Table 2.

Table 2 Stable regions and libration of angles around the given value

Region	ω	ϕ_0	ϕ_2
$(A_0,\ A_1)$	—	—	$(0, \pi)$
$po_2,\ po_3$	π	π	π
po_4	0	π	π
B	—	—	π
$(D_0,\ D_1)$	$(0,\ \pi)$	—	—
$(D_2,\ D_3)$	$(\frac{\pi}{2},\ \frac{3\pi}{2})$	—	—
E	—	π	—

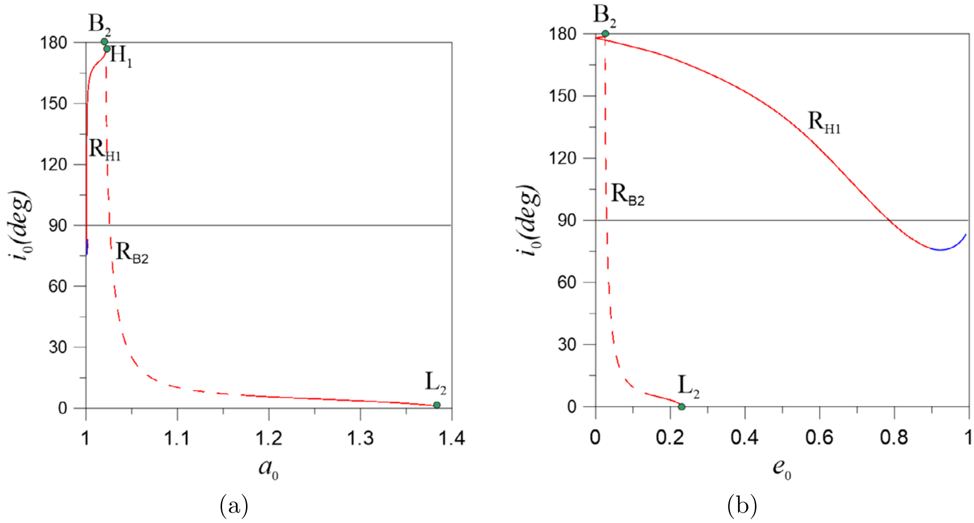

Fig. 7 Families R_{B2} and R_{H1} presented in the planes (a) $a_0 - i_0$ and (b) $e_0 - i_0$. Colors indicate stability as in Fig. 5

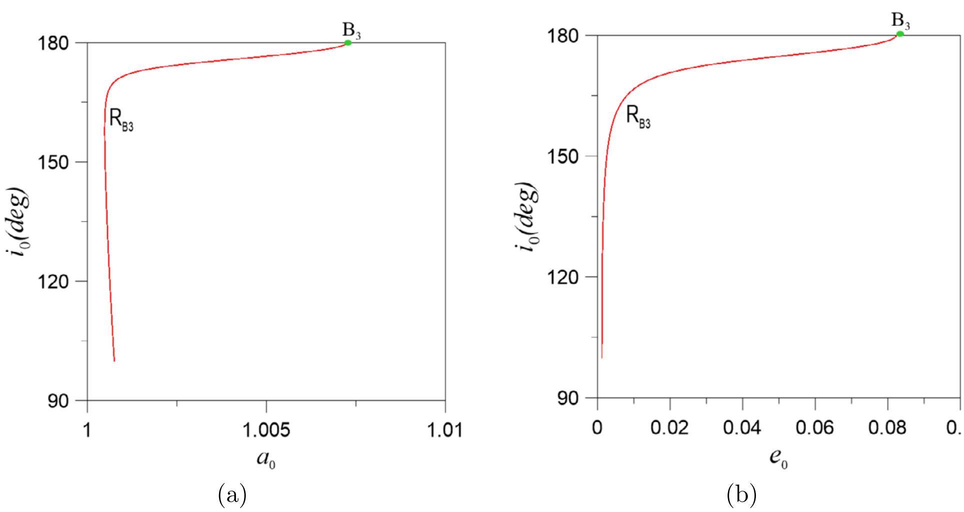

Fig. 8 Family R_{B3} of 3D retrograde symmetric periodic orbits (a) $a_0 - i_0$ and (b) $e - i_0$. All orbits are simply unstable

4.1 The planar case ($i = 180°$)

Concerning motion of mode 2 or 3 our initial conditions, apart from a_0 and e_0 which are defined by the grid, are ($\varpi_0 = \pi$, $M = 0$) or ($\varpi_0 = 0$, $M = \pi$). For the circular problem ($e' = 0$) the dynamical map is presented in Fig. 9. The families of periodic orbits that correspond to circular motion, R_C (mode 0) and R_2 (modes 2 and 3) are also presented with colors indicating their stability. It is clear that horizontally stable orbits are associated with stable regions and unstable ones are surrounded by chaotic regions, although for the R_C family these chaotic regions are very fine to be visible in the map. When we consider the elliptic model, only four isolated periodic orbits exists, denoted by 'po_i', $i = 1, .., 4$. The first is unstable and is located in a chaotic regime, while the rest ones are stable and are located inside stable regions. In these regions all resonant angles and the longitude of perihelion (ϖ) librate. For the regions A_1 (mode-2), only ϕ_2 librates around π. In region C the orbits are almost circular and no librations occur.

For orbits of mode 1 the dynamical maps are presented in Fig. 10. The initial conditions are ($\varpi_0 = 0$, $M = 0$) or ($\varpi_0 = \pi$, $M = \pi$). For the circular case (panel a and b) the characteristic curves of the families R_C and R_1 are also shown. We obtain two large stable regions (for $\varpi = 0$ and $\varpi = \pi$) which are crossed by the horizontally stable family R_1. Stable regions of circular motion also exists around the stable parts of family R_C. All these regions survive also when Jupiter's eccentricity is taken into account (see panel c). The wide stable regions (denoted by A_0) are characterized by librations of resonant angle ϕ_2 around 0.

4.2 The 3D case

By using as a base the maps of planar motion, we set the inclination $i < 180°$ and we get two different configurations for each case (modes-2,3 and mode-1) which are dis-

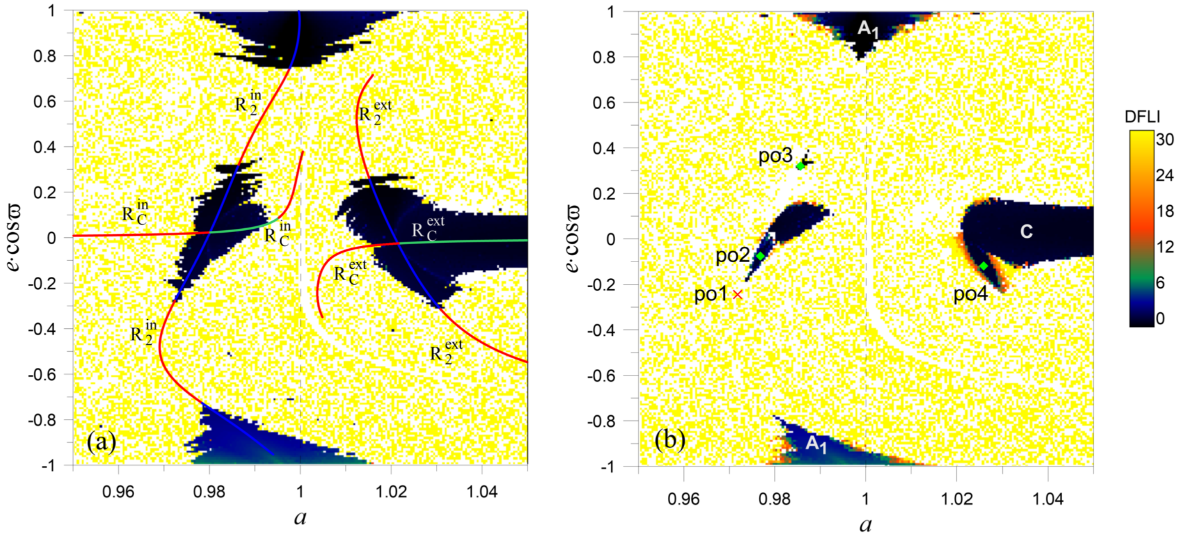

Fig. 9 Dynamical maps for planar motion of mode 2 and 3. (a) planar circular problem (e' =0). The curves presents the relative families of periodic orbits and color indicates the stability as in Fig. 2 (b) the same dynamical map but for the elliptic model ($e' = 0.048$). The existed isolated periodic orbits are denoted by po_i, $i = 1, ..4$

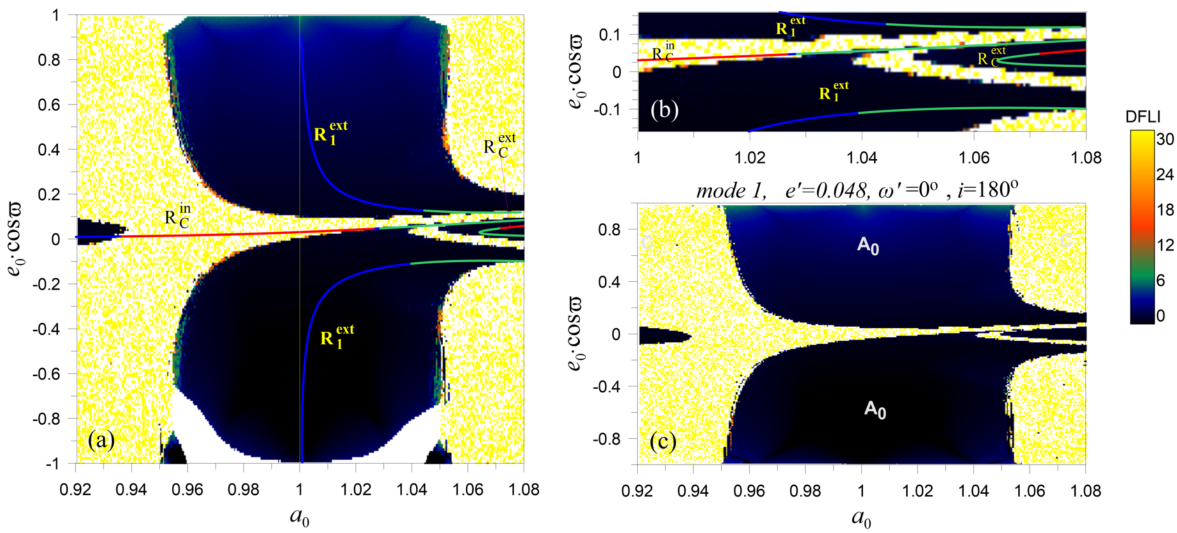

Fig. 10 Dynamical maps for planar motion of mode 1. (a) planar circular problem (e' =0). The curves presents the relative families of periodic orbits and color indicates the stability as in Fig. 2 (b) zoom of an area of panel a. c) Dynamical map for the elliptic model ($e' = 0.048$)

tinguished by the initial value of the mean longitude λ (0 or π). Particularly, we present dynamical maps for the inclinations 178°, 175° and 165° and for all cases we consider the elliptic model ($e' = 0.048$). The different configurations for the initial conditions are presented in Table 3. This problem has also been studied numerically for arbitrary eccentricity of the planet and at the nominal 1/-1 resonance location by (Caritá et al. 2022), and their libration modes at Jupiter's eccentricity are in agreement with our results.

For the case of modes 2 and 3 the dynamical maps are presented in Fig. 11. For $i_0 = 178°$ we can still observe the stable regions A_1 where ϕ_2 librates around π. The same librations are shown in the islands B. The circular orbits almost disappeared but reappear for $i_0 = 175°$. But for this inclination value the most important dynamical feature is the appearence of the stability regions D_0 and D_1 for the configuration $\lambda_0 = \pi$, where ω librates around 0 and π respectively, as in a Kozai resonance. These regions becomes larger for $i_0 = 165°$ and $\lambda_0 = \pi$. Also, a region E appears where the angle ϕ_0 librates around π. Instead, for $\lambda_0 = 0$ chaos dominates but some stable regions (D_2) exist where ω librates around $\pi/2$.

The dynamical maps for orbital configurations of mode-1 are presented in Fig. 12. We observe that the main stable

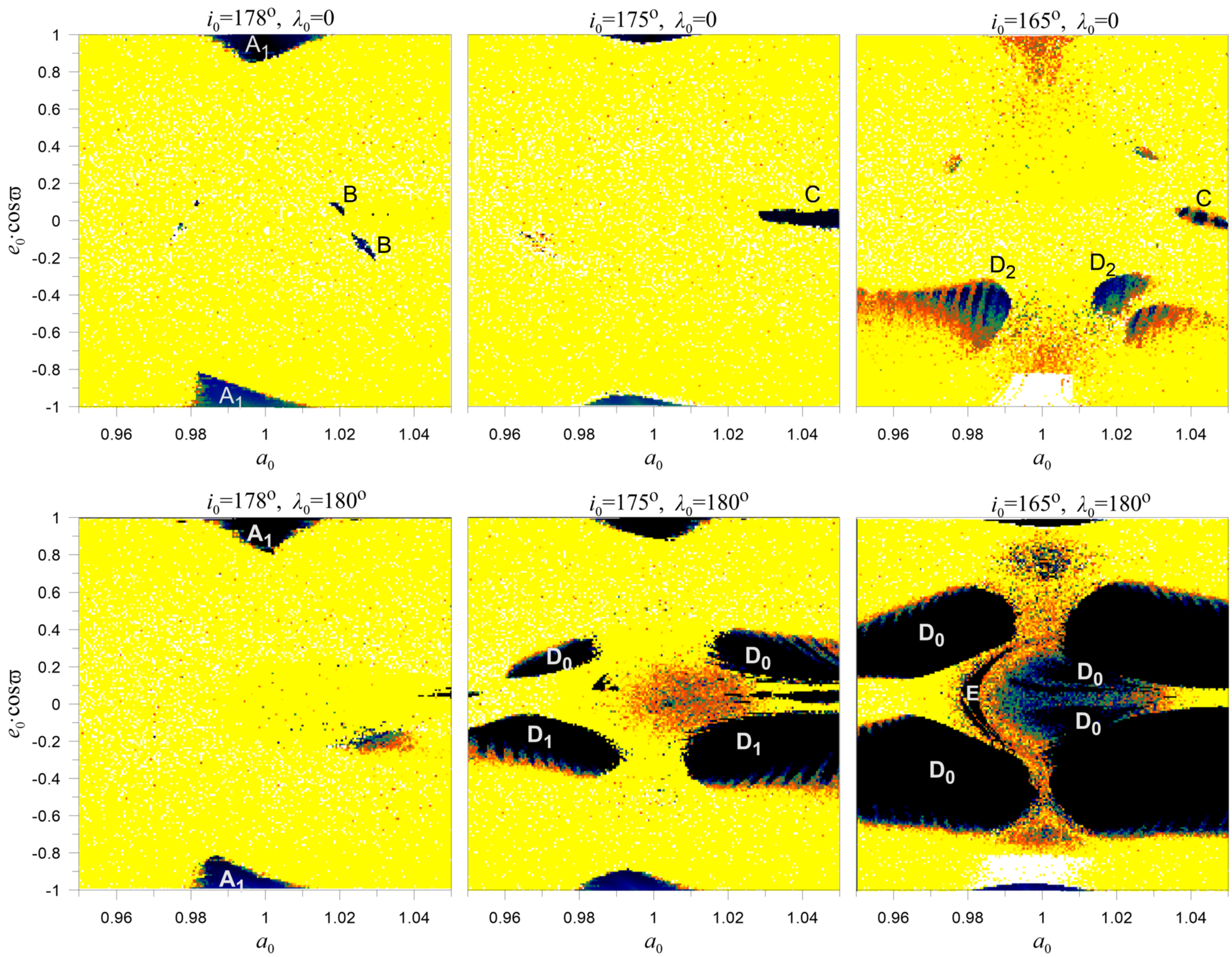

Fig. 11 Dynamical maps for the configurations of modes-2 and 3 and for $\lambda = 0$ (upper panel), and $\lambda = \pi$ (bottom panel)

Table 3 Initial configurations for the dynamical maps of 3D orbits

mode	λ_0	ω_0	Ω_0	M_0
2,3	0	$\pi/2$	$3\pi/2$	0
		$3\pi/2$	$3\pi/2$	π
	π	π	0	0
		0	0	π
1	0	0	0	0
		π	0	π
	π	$\pi/2$	$3\pi/2$	π
		$3\pi/2$	$3\pi/2$	0

regions A_0 that exist in the planar case (see Fig. 10c), also are apparent in the inclined cases but some chaotic zones seems to penetrate them. For $\lambda_0 = 0$, regions with librations of the argument of pericenter ω around 0 and π (regions D_0 and D_1, respectively) are generated. For $i_0 = 175°$, they exist in the exterior area and, for $i_0 = 165°$, appear in the interior area, too. Such librations do not exist for $\lambda_0 = \pi$, where librations of ϕ_2 around 0 dominates. Also we note the region E in the map of $i_0 = 175°$ that shows librations of angle ϕ_0 around π.

5 An application to the asteroid 514107 Ka'epaoka'awela

The asteroid 514107 Ka'epaoka'awela (or 2015 BZ509) is a retrograde co-orbital asteroid of Jupiter (Wiegert et al. 2017; Morais and Namouni 2017a). Long term numerical integrations of clones within the error bars of its fitted orbit show that some exhibit stability over the lifetime of the solar system, while others slowly diffuse towards polar orbits beyond Neptune's orbit, suggesting that it could have been captured from interstellar medium (Namouni and

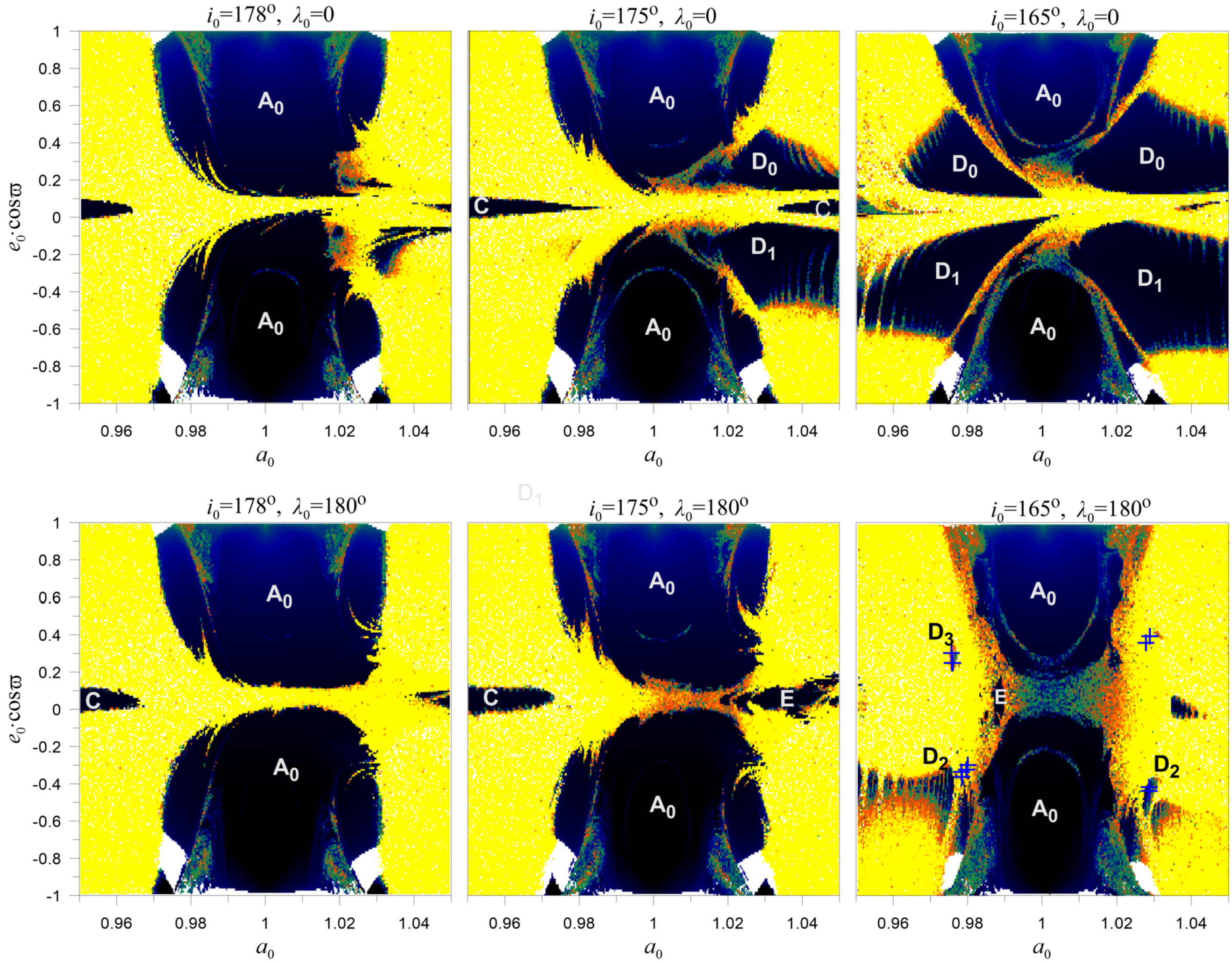

Fig. 12 Dynamical maps for the configuration of mode 1 and for $\lambda = 0$ (upper panel), and $\lambda = \pi$ (bottom panel). The crosses in the bottom-right map indicate potential locations of the asteroid Ka'epaoka'awela (see Sect. 5)

Morais 2018b). Taking its location from NASA JPL's Horizons ephemeris system [1] and considering as reference plane the Jupiter's orbital plane with $\varpi' = 0$ and an epoch where $M' = 0$ the orbital elements of the asteroid are approximately $a/a' = 0.986789$, $e = 0.377$, $i = 164.432°$, $\omega = 257.369°$, $\Omega = 293.805°$ and $M = 216.944°$. By integrating the asteroid's orbit for 2.3Mys we obtain a bounded co-orbital evolution since its mean motion is $n/n' \approx 1$ as it is shown in Fig. 13. At the same figure we obtain that ω switches from rotations to librations in an irregular way but there are significant large time spans where librations takes place either around 0 or π. The resonant angle ϕ_2, although it shows large amplitude librations, there are irregular episodes of circulation. A similar evolution holds for the angle ϕ_0 and it is not shown. We note here that some of the stable clones in (Namouni and Morais 2018a) have $\omega = 0, \pi$ while others have $\phi_2 = 0$ which shows these 2 regions are close in phase space, also in agreement with the numerical results for the CR3BP in (Morais and Namouni 2016).

These orbital features, discussed above, indicate the chaotic nature of the orbit. In the framework of the elliptic RTBP we computed the maximum Lyapunov characteristic exponent (MLCE) after a long time integration in order to estimate the Lyapunov time, t_L (Contopoulos 2002). The corresponding plot is shown in Fig. 14 at which we observe that the MLCE saturates to the value 1.57×10^{-4} and the Lyapunov time, which is the inverse of MLCE is $t_L \approx 6350$ years. This value is typical for prograde inner belt asteroids (Whipple 1995) but, generally, the dynamical life-time of asteroids is quite larger. The case of Ka'epaoka'awela seems to be similar to 522 Helga asteroid which has $t_L = 6900$ years but its orbit is stable for 10 million years, a phenomenon called 'stable chaos' (Milani and Nobili 1992).

[1] https://ssd.jpl.nasa.gov/horizons/.

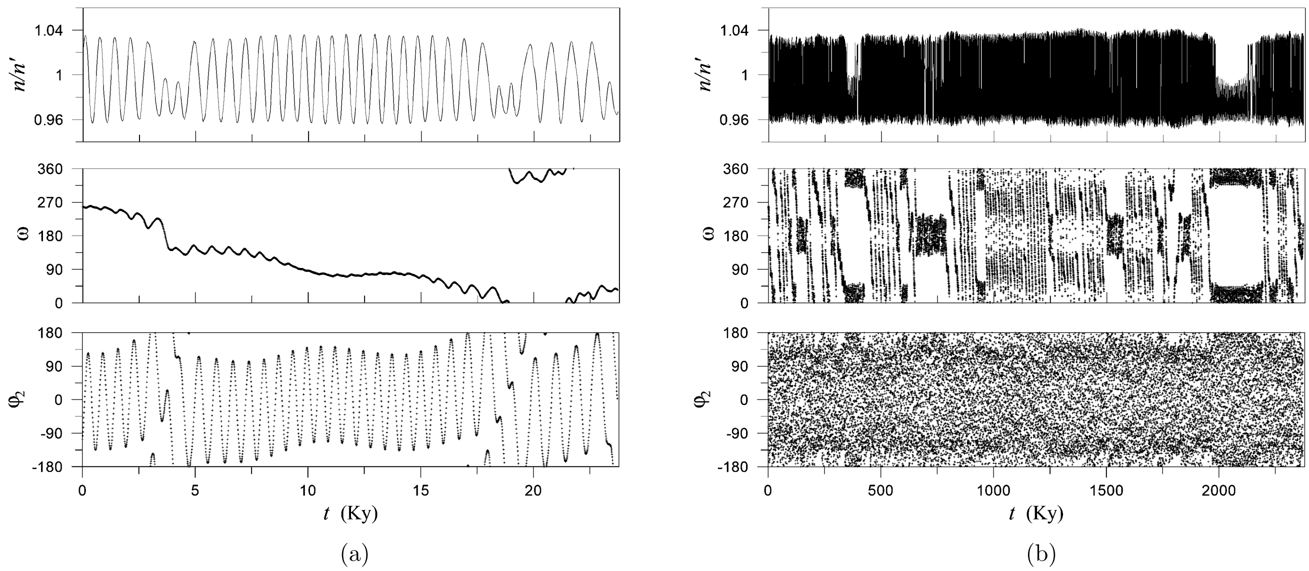

Fig. 13 The evolution of mean motion, argument of pericenter and resonant angle ϕ_2 along the orbit of Ka'epaoka'awela for about a) 20 Kys b) 2000 Kys

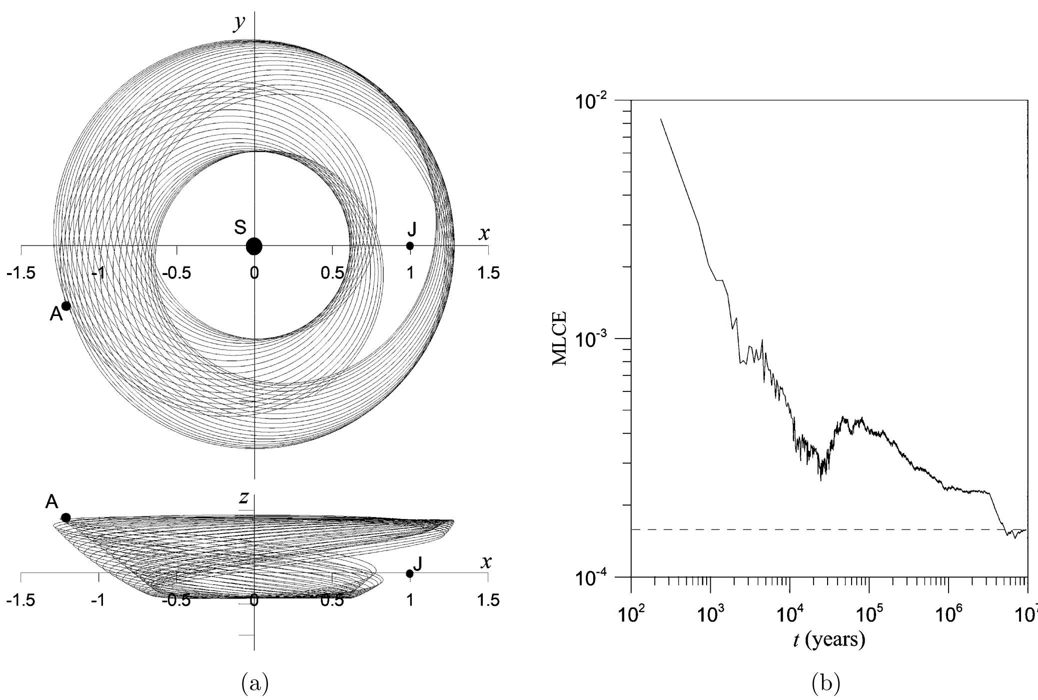

Fig. 14 a) The orbit of Ka'epaoka'awela in the rotating frame for 250 years. Circle A indicates the initial position of the asteroid b) The maximum Lyapunov characteristic exponent after an integration of 10Mys

In order to identify the location of the asteroid with respect to our dynamical maps we identify along the numerical integration, with step the Jupiter's period, the moments when $\psi = \psi_0 \pm \delta\psi$, where ψ indicates the angles, i,ω,Ω and λ and ψ_0 are the values of the particular dynamical map. Figure 14a shows that the orbit has the shape of a "trisectrix" shown in Fig. 1f and dynamically follows the orbital configuration of mode 1 (see also Morais and Namouni 2017a). Therefore we examine the case where ψ_0 corresponds to values of the dynamical maps shown in Fig. 12 for $i = 165^\circ$. The projection of the successive moments on the dynamical maps is shown by crosses in Fig. 12 and are found only for $\lambda = \pi$. Indeed, it is observed that the asteroid evolves in a chaotic sea outside the wide stable regions A_0. However, it passes close to regions D_2 and D_3 where ω librates around $\pm\pi/2$. This is an evidence that evolution is affected by the Kozai-Lidov resonance which is present in the region of 1/-1 resonance as it is shown in Morais and Namouni (2016).

6 Conclusions

In the present paper we studied the dynamics of retrograde 1/-1 mean motion resonance with Jupiter in the framework of the RTBP. We computed families of periodic orbits and dynamical maps of stability in order to classify the various modes of motion that are present.

In the planar model we studied the family of circular retrograde periodic orbits, R_C, which is divided in the interior and the exterior segment (mode-0). The family far from co-orbital motion is stable but when the resonance is approached it becomes unstable and we obtain the bifurcation of the families R_2 (interior and exterior) of elliptic orbits, which for low eccentricities are stable (mode-3). Interior family R_2 continues up to high eccentricities where a stable part exist (mode-2). Exterior family becomes very unstable in moderate eccentricities. Family R_1 is related to mode-1 orbits and shows stable co-orbital periodic orbits of a trisectrix shape in the rotating frame and passes Jupiter twice per period (one inside and one outside Jupiter).

The circular planar family has four vertical critical orbits (v.c.o.). One belongs to the interior part and the three ones to the exterior part. Family R_1 has one v.c.o. From these critical orbits families of 3D retrograde symmetric periodic orbits; these are: R_{A1}, R_{B1}, R_{B2}, R_{B3}, R_{B4}. The first one, R_{A1}, is located at $a < 1$ (interior orbits). All families consist of unstable orbits except for the family R_{B1} which has a stable part for $180° < i < 172.8°$. R_{A1}, R_{B2} and R_{B1} are continued down to $i = 0°$ and terminate to Lagrangian points L_1, L_2 and L_3, respectively. The numerical continuation of R_{B3} stops at $i \approx 100°$ due to strong instability. Finally, the family R_{B4} is connected with an orbit of the family R_{B1} and includes orbits with low eccentricity values ($0.00 < e < 0.11$).

The unstable periodic motion for 3D orbits indicates the existence of wide regions in phase space of chaotic motion. In order to find possible regions of stable motion we computed dynamical stability maps. The grids of initial conditions are defined on the plane $(a - e)$ and chosen in order represent orbits of all modes. It is shown that chaotic regions dominate for modes 2 and 3 but for $i < 170°$ stable regions appears where the argument of pericenter librates. For mode-1 orbital configuration and for the planar case we obtain wide regions of stability where the resonant angle ϕ_2 librates around 0. These regions still exist and dominates for $i < 180°$ around $a = 1$. It is shown, in agreement with previous studies, that the asteroid 514107 Ka'epaoka'awela evolves in orbital mode-1 but outside of the stable area. It is chaotic with relatively short Lyapunov time but does not leave the resonant co-orbital motion for at least 10 Mys.

Author contributions G.V., T.K. and M.H.M. M. wrote the main manuscript. G.V. and T.K. prepared the Figs. 1-14.

Funding information Open access funding provided by HEAL-Link Greece. M.H.M. Morais has financial support from São Paulo Research Foundation (FAPESP/2022/08716-4).

Data availability No datasets were generated or analysed during the current study.

Declarations

Competing interests The authors declare no competing interests.

References

Beaugé, C.: Asymmetric librations in exterior resonances. Celest. Mech. Dyn. Astron. **60**, 225–248 (1994)
Broucke, R.: Stability of periodic orbits in the elliptic, restricted three-body problem. AIAA J. **7**, 1003–1009 (1969)
Caritá, G.A., Signor, A.C., Morais, M.H.M.: A numerical study of the 1/2, 2/1, and 1/1 retrograde mean motion resonances in planetary systems. Mon. Not. R. Astron. Soc. **515**, 2280–2292 (2022)
Contopoulos, G.: Order and Chaos in Dynamical Astronomy (2002)
Froeschlé, C., Lega, E., Gonczi, R.: Fast Lyapunov indicators. Application to asteroidal motion. Celest. Mech. Dyn. Astron. **67**, 41–62 (1997)
Gallardo, T.: Three-dimensional structure of mean motion resonances beyond Neptune. Celest. Mech. Dyn. Astron. **132**, 9 (2020). https://doi.org/10.1007/s10569-019-9948-7
Greenstreet, S., Gladman, B., Ngo, H., Granvik, M., Larson, S.: Production of near-Earth asteroids on retrograde orbits. Astrophys. J. Lett. **749**, 39 (2012)
Hadjidemetriou, J.D.: Periodic orbits of the planetary type and their stability. Celest. Mech. **43**, 371–390 (1988)
Hadjidemetriou, J.D., Ichtiaroglou, S.: A qualitative study of the Kirkwood in the asteroids. Astron. Astrophys. **131**, 20–32 (1984)
Hénon, M.: Vertical stability of periodic orbits in the restricted problem. I. Equal masses. Astron. Astrophys. **28**, 415 (1973)
Hénon, M.: Generating Families in the Restricted Three-Body Problem. Springer, Berlin (1997)
Hou, X.Y., Liu, L.: On Lyapunov families around collinear libration points. Astron. J. **137**(6), 4577–4585 (2009). https://doi.org/10.1088/0004-6256/137/6/4577
Huang, Y., Li, M., Li, J., Gong, S.: Dynamic portrait of the retrograde 1:1 mean motion resonance. Astron. J. **155**, 262 (2018)

Ichtiaroglou, S., Katopodis, K., Michalodimitrakis, M.: Periodic orbits in the three-dimensional planetary systems. J. Astrophys. Astron. **10**, 367–380 (1989)
Jefferys, W.H., Standish, E.M.: Further periodic solutions of the three-dimensional restricted problem. II. Astron. J. **77**, 394–400 (1972)
Kalantonis, V.S.: Numerical investigation for periodic orbits in the hill three-body problem. Universe **6**(6), 72 (2020). https://doi.org/10.3390/universe6060072
Kankiewicz, P., Wlodarczyk, I.: Dynamical lifetimes of asteroids in retrograde orbits. Mon. Not. R. Astron. Soc. **468**, 4143–4150 (2017)
Kankiewicz, P., Wlodarczyk, I.: How long will asteroids on retrograde orbits survive? Planet. Space Sci. **154**, 72–76 (2018)
Kotoulas, T.A., Voyatzis, G.: Planar retrograde periodic orbits of the asteroids trapped in two body mean motion resonances with Jupiter. Planet. Space Sci. **182**, 1–12 (2020a)
Kotoulas, T.A., Voyatzis, G.: Retrograde periodic orbits in 1/2, 2/3 and 3/4 mean motion resonances with Neptune. Celest. Mech. Dyn. Astron. **132**, 33 (2020b)
Kotoulas, T.A., Morais, M.H.M., Voyatzis, G.: The phase space structure of retrograde mean motion resonances with Neptune: the 4/5, 7/9, 5/8 and 8/13 cases. Celest. Mech. Dyn. Astron. **134**(6), 1–25 (2022a)
Kotoulas, T.A., Voyatzis, G., Morais, M.H.M.: Three-dimensional retrograde periodic orbits of asteroids moving in mean motion resonances with Jupiter. Planet. Space Sci. **210**, 1–10 (2022b)
Lara, M., Peláez, J.: On the numerical continuation of periodic orbits. An intrinsic, 3-dimensional, differential, predictor-corrector algorithm. Astron. Astrophys. **389**, 692–701 (2002). https://doi.org/10.1051/0004-6361:20020598
Lei, H.: Three-dimensional phase structures of mean motion resonances. Mon. Not. R. Astron. Soc. **487**, 2097–2116 (2019)
Li, M., Huang, Y., Gong, S.: Survey of asteroids in retrograde mean motion resonances with planets. Astron. Astrophys. **630**, 1–8 (2019)
Milani, A., Nobili, A.M.: An example of stable chaos in the solar system. Nature (London) **357**, 569–571 (1992). https://doi.org/10.1038/357569a0
Morais, M.H.M., Namouni, F.: Asteroids in retrograde resonance with Jupiter and Saturn. Mon. Not. R. Astron. Soc. **436**, 30–34 (2013a)
Morais, M.H.M., Namouni, F.: Retrograde resonance in the planar three-body problem. Celest. Mech. Dyn. Astron. **117**, 405–421 (2013b)
Morais, M.H.M., Namouni, F.: A numerical investigation of coorbital stability and libration in three dimensions. Celest. Mech. Dyn. Astron. **125**, 91–106 (2016)
Morais, H., Namouni, F.: Planetary science: reckless orbiting in the solar system. Nature (London) **543**, 635–636 (2017a). https://doi.org/10.1038/543635a
Morais, M.H.M., Namouni, F.: First trans-neptunian object in polar resonance with Neptune. Mon. Not. R. Astron. Soc. **472**, 1–4 (2017b)
Morais, M.H.M., Namouni, F.: Periodic orbits of the retrograde coorbital problem. Mon. Not. R. Astron. Soc. **490**, 3799–3805 (2019)
Murray, C.D., Dermott, S.F.: Solar System Dynamics (1999). https://doi.org/10.1017/CBO9781139174817
Namouni, F., Morais, M.H.M.: The disturbing function for asteroids with arbitrary inclinations. Mon. Not. R. Astron. Soc. **474**, 157–176 (2018a). https://doi.org/10.1093/mnras/stx2636
Namouni, F., Morais, M.H.M.: An interstellar origin for Jupiter's retrograde co-orbital asteroid. Mon. Not. R. Astron. Soc. **477**, 117–121 (2018b)
Namouni, F., Morais, M.H.M.: An interstellar origin for Jupiter's retrograde co-orbital asteroid. Mon. Not. R. Astron. Soc. **477**, 117–121 (2018c)
Namouni, F., Morais, M.H.M.: Resonance libration and width at arbitrary inclination. Mon. Not. R. Astron. Soc. **493**, 2854–2871 (2020)
Voyatzis, G.: Chaos, order, and periodic orbits in 3:1 resonant planetary dynamics. Astrophys. J. **675**, 802–816 (2008)
Voyatzis, G., Kotoulas, T.: On the retrograde planar co-orbital asteroid motion with Jupiter. In: Lemaitre, A., Libert, A.-S. (eds.) Complex Planetary Systems II: Latest Methods for an Interdisciplinary Approach. Proceedings IAU Symposium, pp. 1–3 (2024). https://doi.org/10.1017/S1743921323003630
Whipple, A.L.: Lyapunov times of the inner asteroids. Icarus **115**, 347–353 (1995). https://doi.org/10.1006/icar.1995.1102
Wiegert, P., Connors, M., Veillet, C.: A retrograde co-orbital asteroid of Jupiter. Nature (London) **543**, 687–689 (2017)